Electronic Supplementary Information (ESI) for

A two-photon fluorescence, carbonized polymer dot (CPD)-based, wide range pH nanosensor: a view from the surface state

Zepeng Huo [a, c], Gang Chen [a], Yijia Geng [a], Lili Cong [a], Lingyun Pan [b], Weiqing Xu [a], Shuping Xu [a,*]

[a] State Key Laboratory of Supramolecular Structure and Materials, Institute of Theoretical Chemistry, College of Chemistry, Jilin University, Changchun 130012, P. R. China

[b] College of Physics, Jilin University, Changchun 130012, P.R. China

[c] Electron Microscopy Center, Jilin University, Changchun, 130012, P. R. China

*Corresponding author

Email: xusp@jlu.edu.cn

CONTENTS:

1. Materials

Catechol with the reagent grade was purchased from Macklin Inc (Shanghai, China). Glutathione (GSH), phenylalanine (Phe), Lysine(Lys), tryptophan (Trp), arginine (Arg), glutamic acid (Glu), metal ions, nigericin, and HEPES (4-(2-hydroxyethyl)-1-piperazineethanesulfonic acid) were all purchased from Aladdin Ltd (Shanghai, China). Ethylenediamine ($C_2H_8N_2$) was purchased from Sinopharm Chemical Reagent Co., Ltd (Shanghai, China). Dulbecco's modified Eagle's medium (DMEM) and FBS were obtained from GIBCO Thermo Fisher Scientific Co. Ltd (Shanghai, China). The WST-1 (2-(4-iodophenyl)-3-(4-nitrophenyl)-5-(2,4-disulfophenyl)-2H-tetrazolium, monosodium salt) assay kit was from Roche(Shanghai, China). All the chemicals were used without further purification.

2. Characterisations

The morphology and size of the samples were observed by (JEM-2100F, Tokyo, Japan) transmission electron microscope (TEM) operating at 200 kV. Photoluminescence (PL) and PL excitation (PLE) spectra were recorded using a SHIMADZU RF-5301PC Spectro-fluorometer. Ultraviolet−visible (UV−vis) absorption spectra were recorded an Ocean Optics USB4000 spectrometer. Powder X-ray diffraction (XRD) data of the CPD were collected on a Japan Rigaku SmartLab X-ray diffractometer with Cu−Ka radiation (λ=1.5418Å, 40kV, 30mA) at 25℃ with a step-scanning in the scan range from 10° to 60°. Fourier-transform infrared spectroscopy (FT-IR) spectra were taken by a Bruker VERTEX 80 V FT-IR spectrometer at room temperature. X-ray photoelectron spectra (XPS) were acquired by the XPS spectrometer (ESCALAB250Xi model, Thermo Fisher Scientific) with a monochromatic Al Kα irradiation source. The PL quantum yield was measured on the FLS920 combined measurement system

equipped with an integrating sphere (Edinburgh Instrument, England). Raman spectroscopy was measured using JY-HR800 micro-Raman spectroscopy with a 532 nm wavelength YAG laser. Zeta-potential measurements were carried out on a Zetasizer Nano ZS90 (Malvern, Worcestershire, U. K).

3. Quantum yield of CPD

The absolute quantum yield of CPD was measured. The FLS920 (Edinburgh Instrument, England) fluorescence spectrophotometer equipped with integrating sphere was employed. CPD aqueous solution was placed in a quartz cuvette for quantum yield testing. Water was selected as the blank solvent for measurement.

4. Calculation formula of TPA cross section (σ)

The two-photon absorption (TPA) cross-section (σ) of CPD (s) at each wavelength and each incident pulse energy was calculated according to Equation (1), and Rhodamine B was used as the reference (r).[1,2]

$$\sigma_s = \sigma_r \frac{F_s \cdot \Phi_r C_r}{F_r \cdot \Phi_s C_s} \qquad (1)$$

Where F is the fluorescence integral area, Φ is the fluorescence quantum yield, C is the concentration of CPD (s) and reference (r).

5. pH switching circles

To show the repeatable pH sensing performance of CPD, we designed a cyclic experiment. The circulation experiment is realized by continuously adjusting the pH of the solution to be tested. The fluorescence intensity of the prepare CPD solution with a pH of 8 was measured as a control for intensity normalization. Then, we dropped an acid solution into the CPD solution to reduce the pH to 2, and then we measured the fluorescence intensity of the solution again. After that,

the pH of the solution was adjusted to 8 again for another fluorescence intensity test. These operations repeated to test the reusability of the CPD. It should be noted that the fluorescence intensity decreases to a certain extent with cycles due to the continuous dilution of the CPD solution.

6. Calculation of pK_a

The fluorescent emission intensity of this nanoprobe was measured in buffers with various pH values. The pH profiles of fluorescence intensity were fitted with the Henderson-Hasselbach equation for the determination of pK_a values.[3]

$$pK_a = \mathrm{pH} - \log\frac{I_{max}-I}{I-I_{min}} \qquad (2)$$

Where I is the fluorescence intensity of the testing compound at a given wavelength, I_{max} and I_{min} are the maximum and minimum limiting values of I, respectively. K_a is the acid dissociation constant.

7. Cell viability assays

A WST-1 (2-(4-iodophenyl)–3-(4-nitrophenyl)–5-(2, 4-disulfophenyl)–2H-, tetrazolium monosodium salt) assay was used to test the cell viability toward the CPD. The MCF-7 cell line was chosen to test cell viability. Firstly, the cells were cultured in a 96-well plate for 24 h. Then, different contents of the CPD were added to the culture medium to co-culture with cells for additional 24 h. After that, 10 μL of the WST-1 solution was added to each well to incubate for 2 h. At last, the optical density values at 450 nm were recorded to calculate cell viability. The cells cultured without any treatment were used as the control group.

8. Data processing for TPF images

Image J software was used to calculate the intensity density of the TPF images. First, the optical

image was converted to 16-bit image. Next, three options in Area, Integrated density, and Mean gray value were set. Then we selected the ROI manager (in the set measurement of analysis) operation panel to read out the values of the three options selected above. Next, the area of the cell was circled by freehand selections one by one. Then, we clicked the measurement option, and the values of the three options (Area, Integrated density, Mean gray value) were presented. Subsequently, the obtained data are extracted and used for t-test analysis.

9. Additional Figures

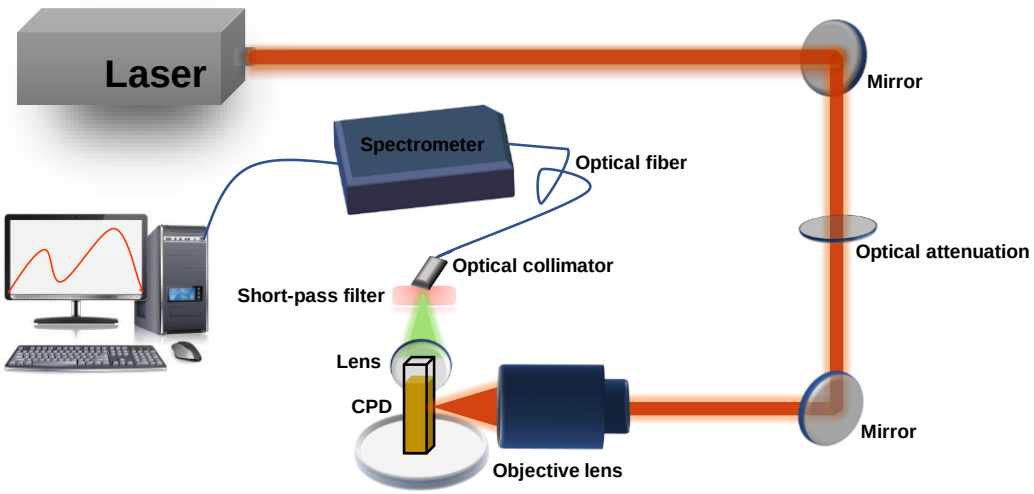

Fig. S1. The setup of the two-photon excited fluorescent measurement system.

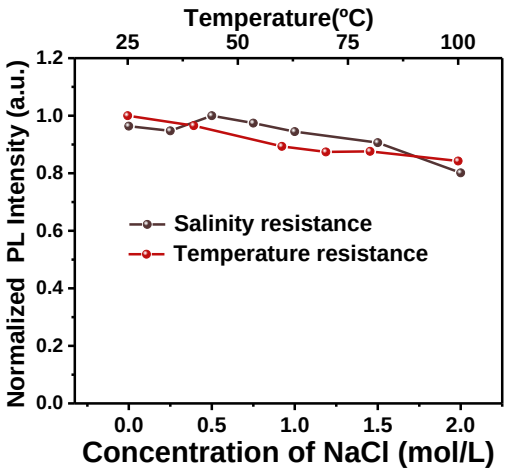

Fig. S2. Effect of NaCl concentration and heating temperature on the PL of the CPD.

The thermal stability of this CPD-based nanosensor was tested. As illustrated in Fig. S1, the CPD exhibit favourable thermal stability in the water phase when the temperature changes from 25 ℃ to 100 ℃ with a 16% decrease of PL intensity.

Furthermore, the CPD in response to different metal ions (Fig. 3f) indicates it has excellent resistance to high ionic strength (Fig. S1), showing high chemical stability, especially in different cell culture mediums.

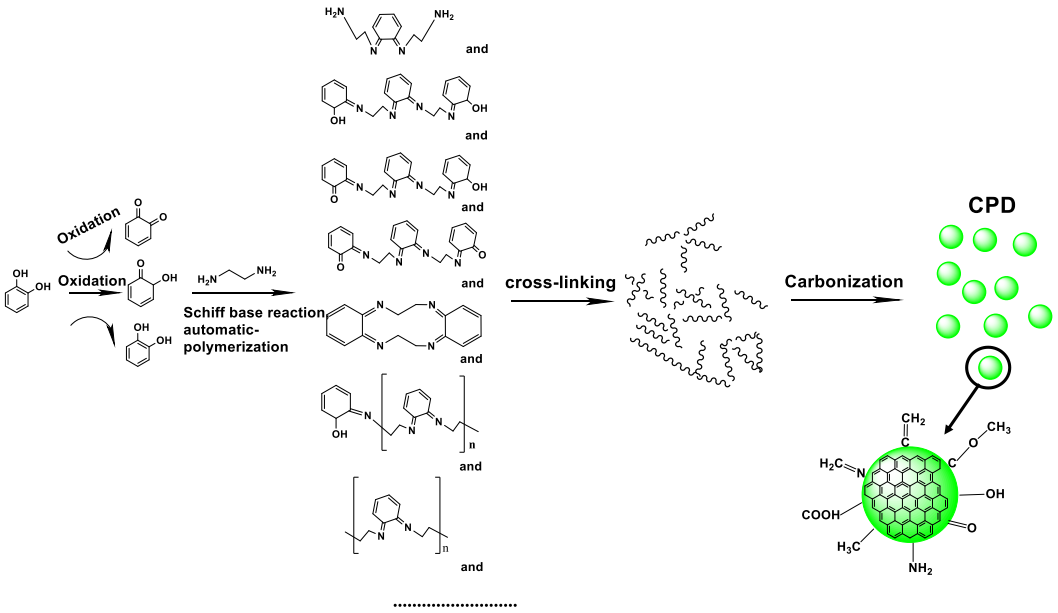

Fig. S3. The formation mechanism of the CPD in the present study.

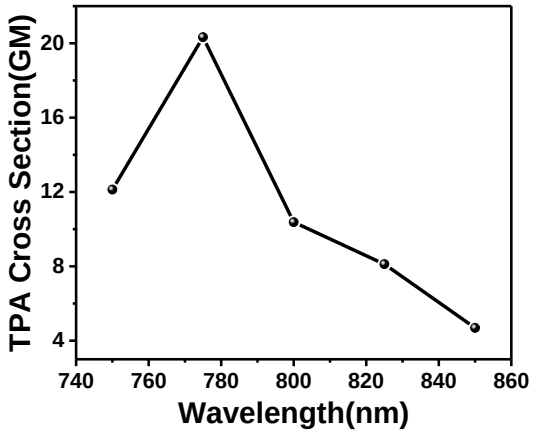

Fig. S4. The TPA cross-section (σ) of the CPD under different excitation wavelengths (Goeppert-Mayer unit, 1GM=10^{-50}cm^{4}s per photon).

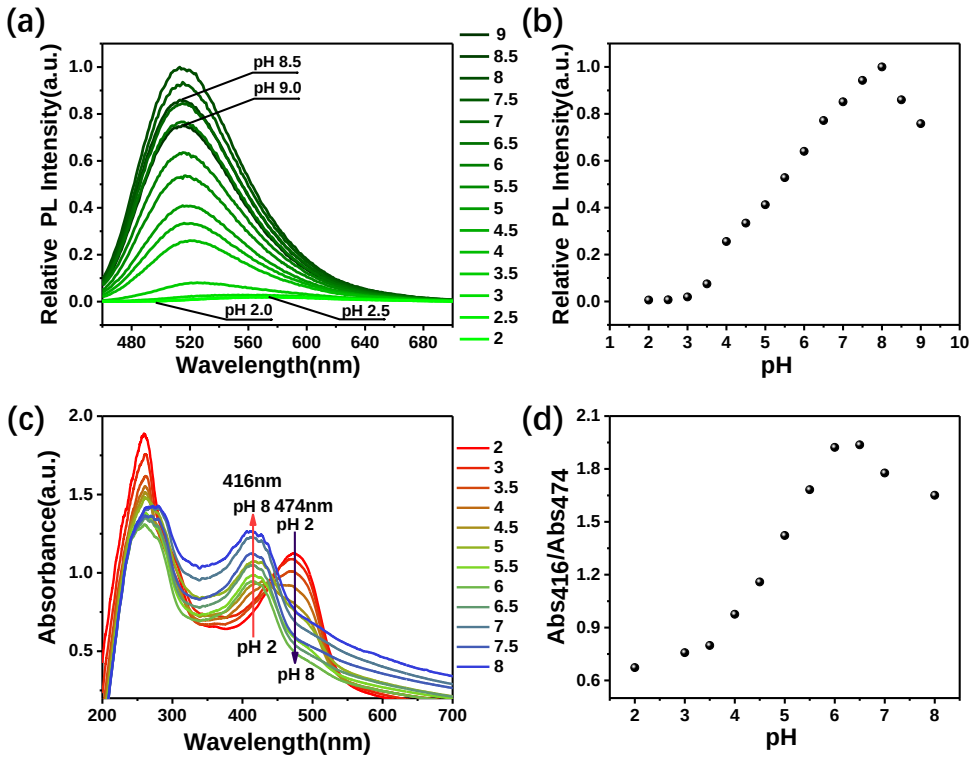

Fig. S5. (a) Relative PL spectra of CPD at various pH values (2.0–9.0). (b) The pH-dependent relative PL intensity evolution, summarized from (a). $\lambda_{ex}/\lambda_{em}$ =420/513 nm. (c)UV-vis spectra of the CPD at various pH values (2.0–8.0). (d) The pH-dependent relative peak intensity (416 nm band /474 nm band) evolution, summarised from (c).

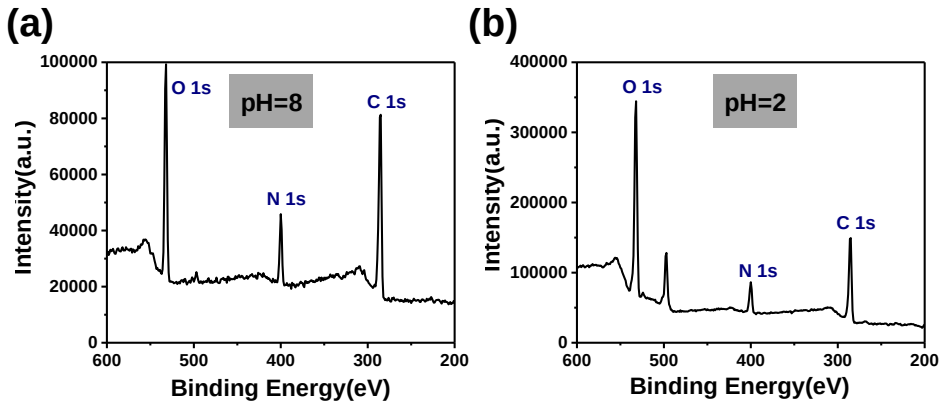

Fig. S6. XPS survey spectra of the CPD under pH=8 or 2.

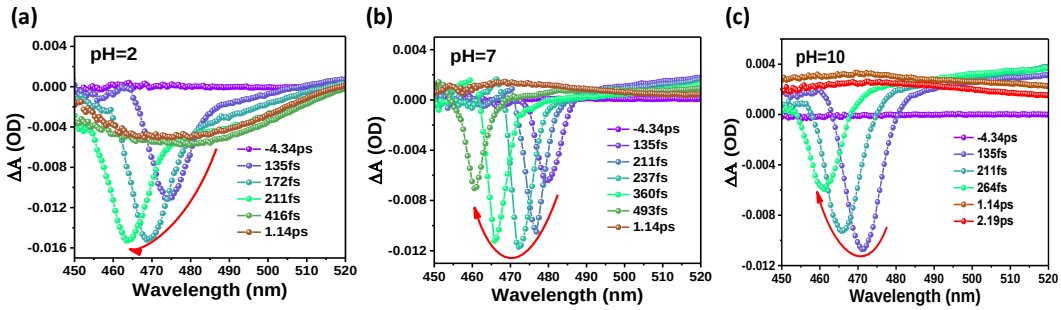

Fig. S7. The excited behaviours of the CPD aqueous solutions under different pH values (a-c: 2, 7 and 10, respectively) with the delay time.

The overall TA spectra under pH=7 in the range of 450 to 500 nm (Fig. S7) can be divided into two stages: (1) within the first 493 fs, the GSB peak significantly increases and blue-shifts, reaching the lowest position at 237 fs. (2) After 493 fs, the time-resolved spectra have no apparent changes, and only very minor evolution occurs up to 1.14 ps.

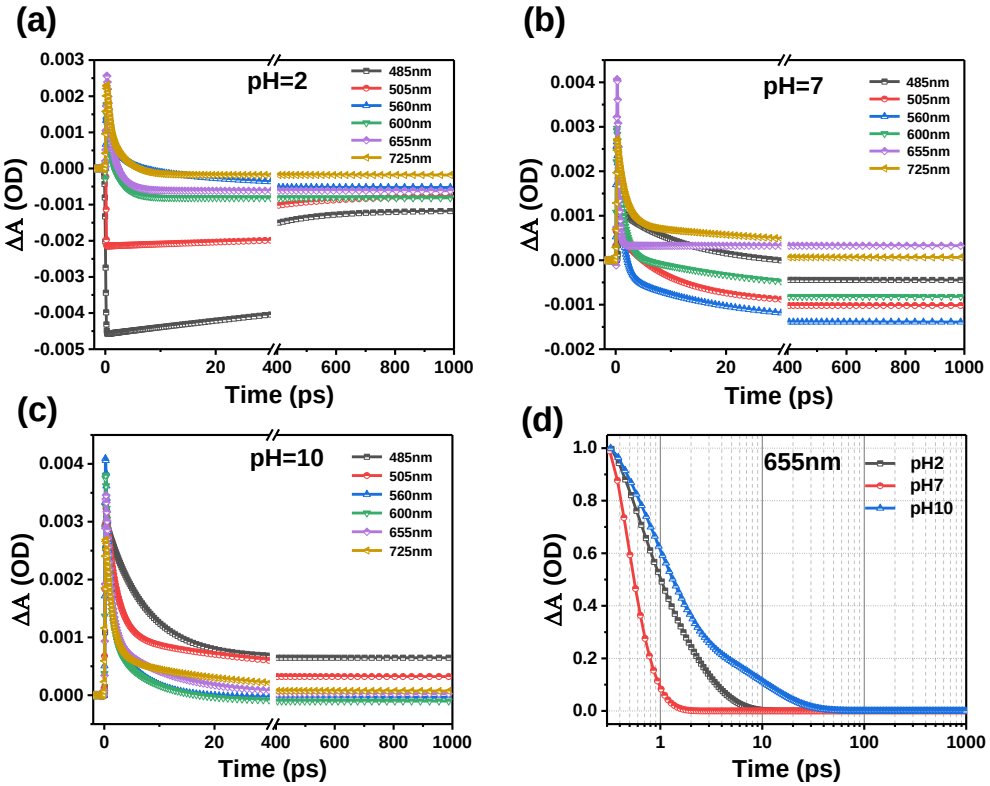

Fig. S8. The excited behaviours of the CPD at different pH values. (a-c) The decay tendencies of the CPD at different wavelengths. (d) Transient decay dynamics of the CPD at 658 nm at

different pH solutions under the 400 nm pulse laser.

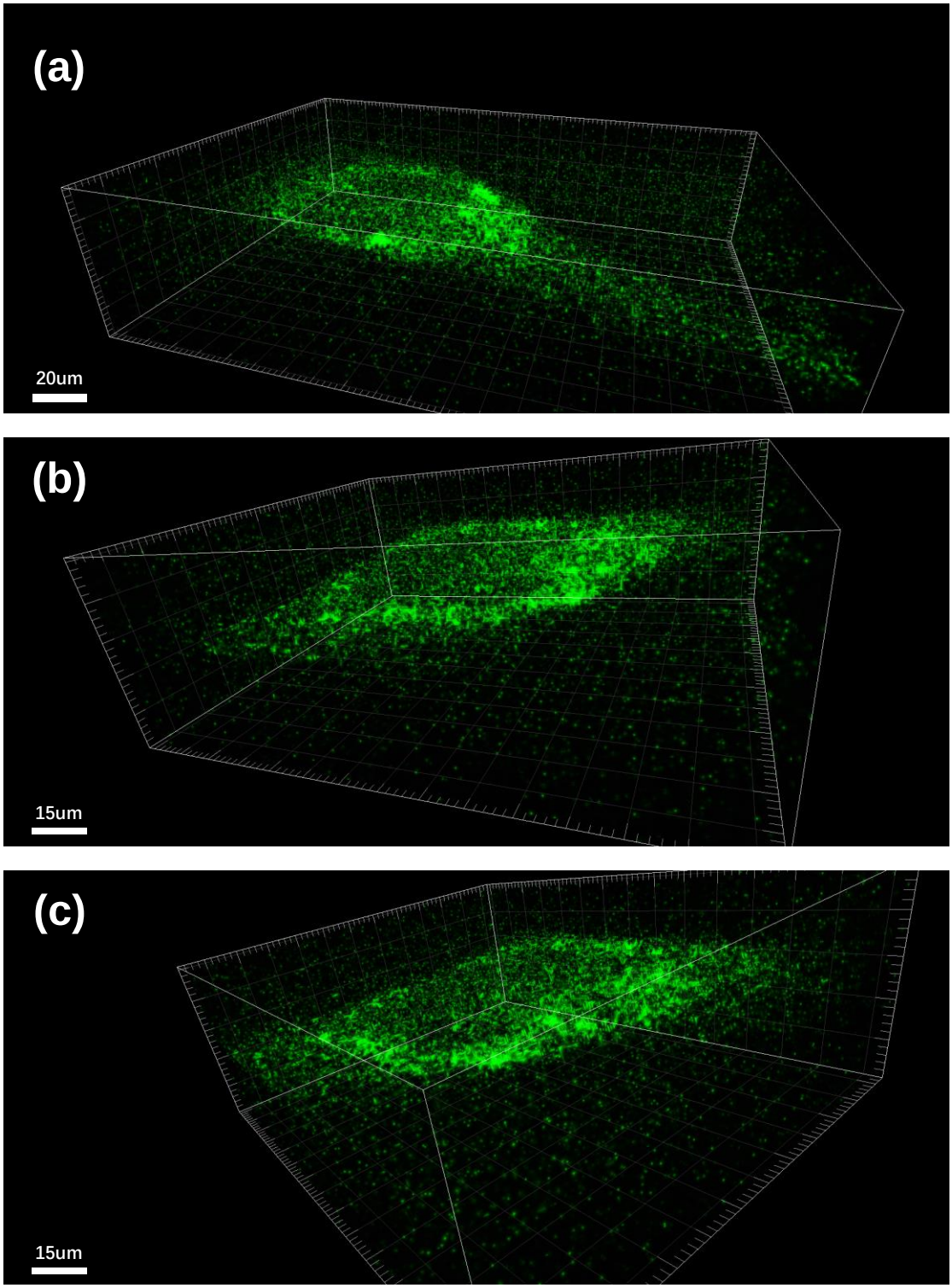

Fig. S9. 3D reconstruction image of cells with the CPD. (a) and (b) are the Z-axis scanning pictures of two cells. (b) and (c) are the same cell viewed from different perspectives.

Table S1 Comparison of the performance of pH-sensitive CDs.

Synthetic materials/ method	**Signal readout**	**Range**	**Sensing mechanism**	**Application**	**Ref**
p-Phenylenediamine and thiourea/ Hydrothermal synthesis	PL	4.0-7.4	protonation and deprotonation of the amino groups on the surface of CDs	pH in live cells and organisms.	4
1,2,4-Triaminobenzene dihydrochloride and urea/ Hydrothermal synthesis	PL	5.0-9.0	azo group and its transformation of a quinoidal form	pH monitoring on the wound	5
m-Phenylenediamine, C_2H_5OH, and H_2SO_4/ Solvothermal method	PL	6.0–10.0	the photoinduced electron transfer	pH in live cells	6
p-Phenylenediamin, o-phenylenediamine, and dopamine/ Hydrothermal synthesis	PL, TPF	3.5 – 6.5	The aggregation conversion of individual CDs	pH in living cells, tissues and zebrafish	7
p-phenylenediamine and $FeCl_3$/ Hydrothermal synthesis	PL	4.0–6.0	Regulation of the surface state of CDs	pH in live cells	8
Basic fuchsin and citric acid monohydrate/Hydrothermal synthesis	PL	5.0 – 8.0	not given	pH in live cells	9
Ethanediamine and catechol/ Hydrothermal synthesis	PL, TPF, & ratiometric	3.0-8.0, 3.5-6	Regulation of the surface state of CDs	pH in live cells	This work

Note: TPF; two-photon fluorescence

19. References

1 H. Wang, J. Wei, C. Zhang, Y. Zhang, Y. Zhang, L. Li, C. Yu, P. Zhang and J. Chen, *Chin. Chem. Lett.*, 2020, **31**, 759-763

2 G. Tong, J. Wang, R. Wang, X. Guo, L. He, F. Qiu, G. Wang, B. Zhu, X. Zhu and T. Liu, *J. Mater. Chem. B*, 2015, **3**, 700-706.

3 S. Zhang, G. Chen, Y. Wang, Q. Wang, Y. Zhong, X. F. Yang, Z. Li and H. Li, *Anal. Chem.*, 2018, **90**, 2946-2953.

4 P. Gao, J. Wang, M. Zheng and Z. Xie, *Chem. Eng. J.*, 2020, **381**, 122665.

5 P. Yang, Z. Zhu, T. Zhang, W. Zhang, W. Chen, Y. Cao, M. Chen and X. Zhou, *Small*, 2019, **15**, 1902823.

6 Q. Wang, H. Yang, Q. Zhang, H. Ge, S. Zhang, Z. Wang and X. Ji, *Microchim. Acta*, 2019, **186**, 468.

7 X. Ye, Y. Xiang, Q. Wang, Z. Li and Z. Liu, *Small*, 2019, **15**, 1901673.

8 J. Xia, S. Chen, G. Y. Zou, Y. L. Yu and J. H. Wang, *Nanoscale*, 2018, **10**, 22484-22492.

9 J. Shangguan, D. He, X. He, K. Wang, F. Xu, J. Liu, J. Tang, X. Yang and J. Huang, *Anal. Chem.*, 2016, **88**, 7837-7843.